ARTICLES
https://doi.org/10.1038/s41564-018-0123-9
nature microbiology

Nutritional preferences of human gut bacteria reveal their metabolic idiosyncrasies

Melanie Tramontano[1,8], Sergej Andrejev[1,8], Mihaela Pruteanu[1,6], Martina Klünemann[1], Michael Kuhn[1], Marco Galardini[2], Paula Jouhten[1], Aleksej Zelezniak[1,7], Georg Zeller[1], Peer Bork[1,3,4,5*], Athanasios Typas[1*] and Kiran Raosaheb Patil[1*]

Bacterial metabolism plays a fundamental role in gut microbiota ecology and host–microbiome interactions. Yet the metabolic capabilities of most gut bacteria have remained unknown. Here we report growth characteristics of 96 phylogenetically diverse gut bacterial strains across 4 rich and 15 defined media. The vast majority of strains (76) grow in at least one defined medium, enabling accurate assessment of their biosynthetic capabilities. These do not necessarily match phylogenetic similarity, thus indicating a complex evolution of nutritional preferences. We identify mucin utilizers and species inhibited by amino acids and short-chain fatty acids. Our analysis also uncovers media for in vitro studies wherein growth capacity correlates well with in vivo abundance. Further value of the underlying resource is demonstrated by correcting pathway gaps in available genome-scale metabolic models of gut microorganisms. Together, the media resource and the extracted knowledge on growth abilities widen experimental and computational access to the gut microbiota.

The composition of the human gut microbiota is closely connected to both health and disease[1–4]. It is influenced by several host factors including the immune system and lifestyle, but also by metabolic cross-feeding among different bacterial species[1,5,6]. Interactions of the microbiota with the host are often mediated by bacterial metabolites such as vitamins, short-chain fatty acids (SCFAs), amino acids, neurotransmitters, and virulence factors and toxins[4,7,8]. For example, specific gut bacteria can cause elevated serum levels of branched-chain amino acids that correlate with insulin resistance in non-diabetic individuals[9]. Several community members, such as *Bacteroides thetaiotaomicron*, are known to be capable of metabolizing complex substrates such as mucin, which is critical for understanding their contribution to inflammation and infection through, for example, weakening of the mucosal barrier[10].

To examine the metabolic capacity of the gut microbiota and dissect complex metabolic interactions, advanced culture-based model systems are urgently needed. However, most gut bacterial species have so far been grown in complex media of unknown chemical composition, and defined or minimal media have been described only for a handful of species[11–16]. This severely limits mechanistic investigations into community functions—for example, discovering cross-fed metabolites or linking functional metabolites to the producer species[17]. Moreover, computational efforts to reconstruct species and community-level metabolic models critically rely on the availability of defined growth media[15,18,19]. Consequently, the mechanistic link between diet or inter-species interactions with microbiota composition and dynamics is currently difficult to establish. To address this, here we report growth profiles of a large, phylogenetically representative panel of human gut bacteria across 4 rich (undefined) and 15 defined media. This has allowed us to characterize their nutritional preferences, accurately map their biosynthetic capabilities, discover metabolic features of several bacteria, and contextualize growth characteristics in terms of gut microbiota ecology.

Results

Selection of representative gut bacterial species. To cover a wide range of phylogenetically as well as metabolically diverse representatives of a healthy human gut microbiota, we selected a total of 96 bacterial strains from 72 species. First, 95 species commonly occurring within the human population—meeting the criteria of relative abundance of 1% or more in at least one sample and a prevalence of more than 10%—were preselected from published metagenomics datasets collected in four countries from a total of 364 healthy humans (Fig. 1b, Supplementary Fig. 1 and Methods). From these, 58 cultivable bacterial strains from 45 species—preferably isolated from human samples and with publicly available and annotated genomes—were selected. We further added 13 probiotics from the genera *Lactobacillus* and *Lactococcus*, 13 pathogens (from the genera *Salmonella*, *Shigella*, *Vibrio*, *Yersinia* and enteropathogenic *Escherichia*), three *Fusobacterium* strains linked to colorectal cancer and inflammatory bowel disease (IBD)[20,21], two strains commonly causing foodborne diseases (*Clostridium perfringens*)[22], *Eggerthela lenta* and *Actinomyces odontolyticus* often associated with abdominal sepsis or bacteraemia[23,24], and one additional representative of three abundant genera (*Coprococcus*, *Eubacterium* and *Prevotella*). Finally, to increase the coverage of metabolic diversity, we additionally selected two species, *Clostridium saccharolyticum* and *Pseudoflavonifractor capillosus*, which were available in culture collections and formed separate metabolic clusters representing reactions not covered by the other selected species (Methods).

[1]European Molecular Biology Laboratory, Heidelberg, Germany. [2]EMBL-EBI, Wellcome Trust Genome Campus, Cambridge, United Kingdom. [3]Max-Delbrück-Centre for Molecular Medicine, Berlin, Germany. [4]Molecular Medicine Partnership Unit, Heidelberg, Germany. [5]Department of Bioinformatics, Biocenter, University of Würzburg, Würzburg, Germany. [6]Present address: Humboldt University Berlin, Berlin, Germany. [7]Present address: Chalmers University of Technology, Gothenburg, Sweden. [8]These authors contributed equally: Melanie Tramontano and Sergej Andrejev.
*e-mail: bork@embl.de; typas@embl.de; patil@embl.de

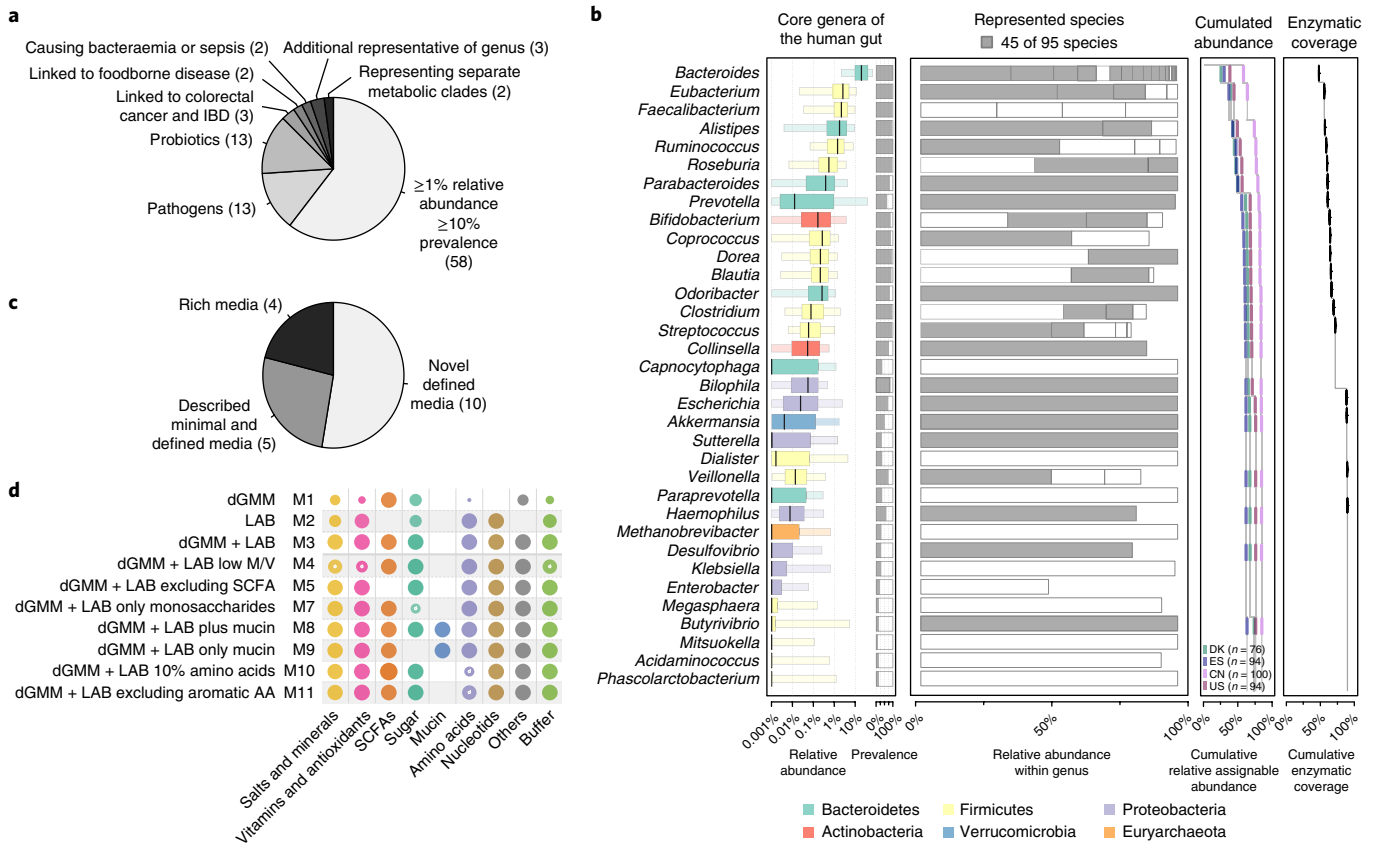

Fig. 1 | Species and media selection. a, Overview of selected bacterial strains. The numbers of selected strains in different categories are shown in parentheses. **b**, Species core of the human gut microbiome based on faecal metagenomes collected from 364 healthy individuals in four countries (DK, Denmark; ES, Spain; CN, China; US, USA) and their representation in this resource (Methods). Boxplots show selected core species grouped by genus (classified using a universal marker gene method[50]) and coloured by phylum; the inner box indicates the inter-quartile range, with the median as black vertical line; the outer bars extend to the 5th and 95th percentiles. Prevalence of individual genera across 364 metagenomics datasets is depicted in grey on the right within the same panel. Species diversity across 364 metagenomics datasets within each genus and their relative abundances are depicted in the middle panel with grey boxes indicating species represented in this screen. Cumulative fraction of relative abundance of represented species normalized by the total assignable metagenomics read abundance is shown in the coloured right panel for each country separately (see inset). The last panel shows cumulative enzyme coverage relative to the core microbiome. **c**, Overview of selected growth media. The numbers of media in different categories are shown in parentheses. **d**, Comparison of nutrient group representation across all newly compounded media. Circle size correlates linearly with the quantity of the respective nutrient group. Changes in media M4–M11 compared to the basis medium M3 dGMM + LAB are additionally marked with a white dot.

The final species collection (Supplementary Table 1) thus represents not only highly abundant and prevalent genera but also important species linked to colorectal cancer, IBD, infectious diseases and taxa of beneficial probiotics (Fig. 1a). For seven of the selected species, genomes were sequenced and assembled in this study (Methods and Supplementary Table 1). Overall, the selected bacteria represent a cumulative enzyme coverage, at EC level 4, of close to 90% when mapping to 364 human gut metagenomes of healthy individuals and cumulative abundance coverage of 72% on average across metagenomics datasets (Fig. 1b and Methods).

Media selection and design. For the vast majority of the selected 96 strains, neither growth characterization data nor defined growth media were previously available. To our knowledge, only 7 defined or minimal media had so far been established for a subset of these, namely for *Escherichia coli* and other enterobacteria[11], *Bacteroides thetaiotaomicron*[12], *Veillonella parvula*[14], *Clostridium perfringens*[13], *Bacteroides caccae* and *Lactobacillus rhamnosus*[15], and other *Bacteroides* species[16].

To enable detailed metabolic characterization of all 96 strains, we designed several defined media by taking into account various known metabolic requirements of gut bacterial species. First, we developed a chemically defined version of the gut microbiota medium (GMM[25]) by excluding all non-defined compounds such as yeast and meat extract. Another defined medium was prepared by combining the Zhang-Mills-Block 1[26] and a chemically defined medium described previously[27] supporting growth of various lactic acid bacteria (hereafter referred to as LAB medium). A mixture of the defined GMM (dGMM) and the LAB medium supplemented with 1 g l^{-1} lactose, 0.5 mg l^{-1} hemin and 2 mg l^{-1} ß-NAD, named dGMM + LAB, formed the basis for all other newly compounded media. These were obtained by excluding either SCFA or aromatic amino acids, by lowering the amounts of minerals and vitamins or by reducing the amounts of amino acids to 10%. Three more media either contained additional mucin, mucin as the sole carbohydrate source, or monosaccharides as carbohydrate source (Fig. 1d and Supplementary Table 2). We further expanded the media set by including defined and minimal media (MM) previously described for *Bacteroides thetaiotaomicron*, *Clostridium perfringens* and *Veillonella parvula*[12–14] and two modified versions of the *E. coli* MM (Fig. 1c and Supplementary Table 2). The initial pH of all defined media was set to 7, which is in the range of the small intestines and the colon[28].

To allow for the growth of more fastidious organisms, four undefined rich media used for cultivation of gut microbial communities or individual species were also included: GMM[25], mGAM[29] (modified Gifu anaerobic medium broth, HyServe), WCA (Wilkinson Chalgren anaerobic agar, Sigma-Aldrich) and BHI (brain heart infusion broth, Sigma-Aldrich) supplemented with 0.5 mg l^{-1} hemin and 2 mg l^{-1} ß-NAD (BHI++). Together, our final set consisted of 15 defined and 4 rich media (Fig. 1c).

Growth profiles reveal complex evolution of nutritional preferences. We evaluated the selected 96 strains for their growth performance across all 19 media. All cultivations were carried out under anaerobic conditions and growth was monitored by measuring optical density (OD at 578 nm) for up to 48 hours (Methods and Supplementary Tables 3 and 4). To ensure that the observed growth was not due to nutrient carryover during inoculation, we tested 55 of the 96 strains for their capability to consistently grow, in all tested media, for three passages (Methods). Notably, we observed reproducible growth (or no growth) between passages 1 and 3 for over 93% of the cases (Supplementary Fig. 2). In many of the remaining cases, the OD measurements (in either passages 1 or 3) were on the threshold of what we considered as growth (maxOD ≥ 0.15; Methods). Furthermore, the cases where we observed discrepancy between the passages are neither restricted to fastidious species or to minimal media. These results, together with the high degree of reproducibility, show that the nutrient carryover from pre-inoculations in rich media had no or only a marginal effect.

Notably, the vast majority of strains, 76 out of 96, grew in at least one defined medium. The median number of growth-enabling media across different species is 10, and the median number of species supported across different media is 51 (Fig. 2a–c). Altogether, our media set allowed growth of phylogenetically as well as functionally diverse gut bacteria in complex as well as defined media.

For 30 species, we also measured the pH after 48 hours of cultivation (Methods). As expected, most species acidified media, with the extent of decrease in pH being inversely proportional to the observed growth (Supplementary Fig. 3). Some species also increased pH, especially in rich media (Supplementary Fig. 3), indicating peptide/protein utilization. Further analysis of pH dynamics across a larger set of strains and media may thus provide additional insights into the basic physiology of gut microorganisms.

Fastidious behaviour was observed for many species. Interestingly, this is not confined to any particular phylogenetic division: 19 strains growing in four or less media are from 13 different genera (six phyla), while other tested members of the same genera act more like generalists showing growth in five or more media. For example, while one out of five *Bifidobacterium* strains tested, *B. animalis* subsp. *lactis* BL-04, is clearly fastidious growing only in the four rich media, the remaining four strains (*B. longum* subsp. *longum*, *B. animalis* subsp. *lactis* BI-07, *B. longum* subsp. *infantis* and *B. adolescentis*) grew in six to thirteen different (including defined) media. Such divergent growth patterns are observed across most genera. In case of *Bacteroides*, the most represented genus in this study, *B. coprocola*, *B. eggerthii* and *B. uniformis* HM-715 grew only in rich or specialized media. In contrast, other *Bacteroides* species grew in several minimal or defined media, in addition to all four rich media. A particularly generalist behaviour was observed for *B. fragilis* and *B. vulgatus* HM-720, which grew in ten defined media. Conversely, similar growth patterns were found between higher taxonomic ranks. For example, *Akkermansia muciniphila* and *Ruminococcus torques* displayed a noticeably similar growth pattern in our screen. Although from different phyla, both species were growing almost exclusively under two particular defined media that contained mucin. Indeed, these two species have previously been described to compete for a similar ecological niche in the mucus layer[30]. Overall, growth patterns that reflect phylogenetic similarity, as well as those implying parallel or convergent evolution towards the same metabolic niche, are both apparent across most taxonomic clades from order to strain level (Fig. 2d,e; Supplementary Fig. 4).

In vitro growth correlates with abundance in the human gut microbiome. We next analysed growth characteristics of bacteria in the context of their standing in the gut microbiota community. For this, we correlated the growth capacity of the species (maximum OD reached) in each of the 19 media with their abundance in the gut metagenomes of each of the 364 healthy individuals (Methods). Several of the tested media showed a significant positive correlation (Fig. 3a). Among these, mGAM and M4 displayed the highest frequency of positive correlations suggesting that these might more closely mimic growth conditions, in terms of nutrients used by bacteria, in the gut. This hypothesis, although difficult to test, is of high practical relevance: the media with good correlations offer a basis for in vitro mechanistic studies wherein growth-rate dependent effects[31] would be reduced. Indeed, mGAM had been reported to reflect the complexity of gut communities after cultivation[29,32].

Furthermore, as many as 11 species grow better in defined media than in rich (Fig. 3b and Supplementary Table 7), and within defined media show stronger growth than most other bacteria (Supplementary Fig. 5). We hypothesize that the metabolic robustness of these species would enable survival in nutrient-low environments. Indeed, we find that these species are more prevalent in the gut metagenomes of healthy individuals (Methods), probably representing diverse gut environments with different nutrient limitations (Fig. 3c).

SCFAs and amino acids inhibit growth of several gut bacteria. Our screen also allowed us to assess the inhibitory effects of SCFAs and amino acids, known to influence microbiome dynamics. SCFAs, especially acetate, propionate and butyrate, are major by-products of complex carbohydrate breakdown processes carried out by the gut bacterial community[33]. SCFAs play a major role in bacterial cross-feeding, but are also linked to various host health conditions[34]. Furthermore, SCFAs have been reported to be toxic to some species at low pH[35,36]. We observed that several species are also affected in our screen wherein the starting pH was circumneutral. Physiological levels of SCFA affected growth of 15 species (Fig. 4a and Methods) in comparison to growth in standard dGMM + LAB medium. While SCFAs boosted the growth of one species (*Lactobacillus vaginalis*), their presence considerably inhibited several phylogenetically diverse gut bacteria (Fig. 4a). To our knowledge, the growth inhibition of these species by SCFAs has not been described before. In future, it would be interesting to study the effect of pH on these inhibitory interactions. We also evaluated the inhibitory effect of amino acids on growth, as several gut commensals are known to be sensitive to (specific) amino acids[37]. We identified three strains, *B. clarus*, *B. xylanisolvens* and *P. merdae*, being sensitive to presence of aromatic amino acids while other species, such as *C. perfringens* C36 and several *Lactobacillus* species, depended on these amino acids for robust growth (Fig. 4a). Furthermore, the growth of most tested species is negatively affected when total amino acid levels were reduced by 90%. In contrast, *Blautia obeum* exhibited increased growth following amino acid reduction (Fig. 4a). This species also generally shows better growth in defined media than in rich, and prefers media with nutrient exclusions (Fig. 2a), suggesting sensitivity towards nutrient excess in general.

Growth promotion by mucin. Only about a dozen species from four genera have, to our knowledge, so far been described as mucin degraders[38]. Within our screen, a much larger number of species thrived in the presence of this biopolymer. The growth of 19 species was boosted in media supplemented with mucin (M8 hits) and 15 species could survive with mucin as the sole carbohydrate source

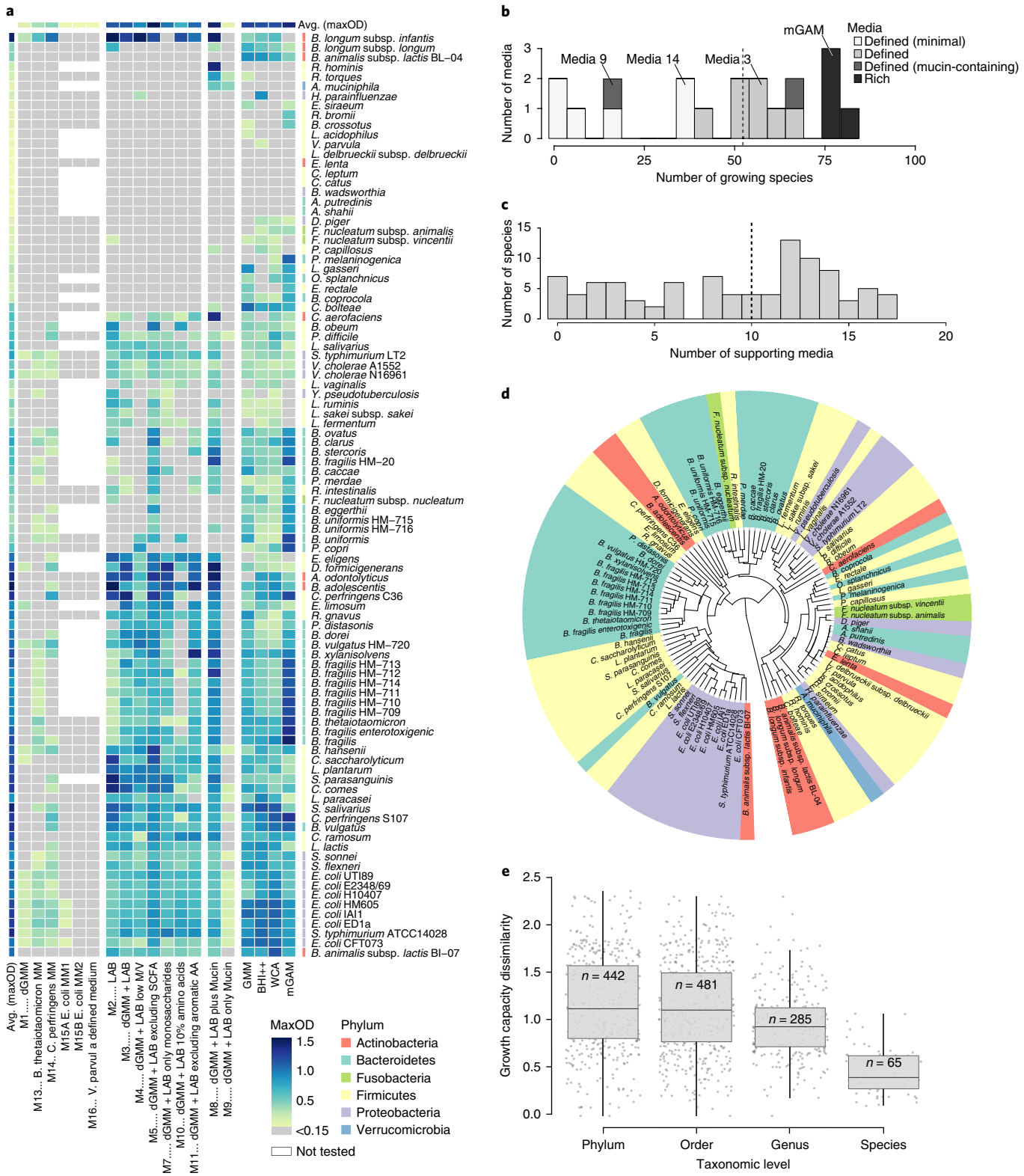

Fig. 2 | Growth profiles of 96 gut bacterial strains across 19 media. a, Heat map showing the growth capacity of 96 gut bacterial strains across minimal (M1, M13–M16), defined (M2–M11) and rich media (GMM, BHI++, WCA and mGAM). The values shown are averages of maximum OD reached in the respective media (Methods and Supplementary Tables 4 and 5). The median number of biological replicates is 5. The exact number of replicates for each strain–media combination is reported in Supplementary Table 5. **b**, Growth-supporting capacity of 19 tested media; median shown as dotted grey vertical line. **c**, Media preference frequency for 96 tested bacteria; median shown as dotted grey vertical line. **d**, Clustering of tested gut bacteria by their growth profiles across 19 media (Methods). Colours mark different phyla. **e**, Distribution of growth capacity dissimilarity (maxOD; Euclidian distance) within different taxonomic ranks. Boxplots show the interquartile range (IQR), the median value and whiskers extending to include all the values less than 1.5 × IQR away from the 1st or 3rd quartile, respectively.

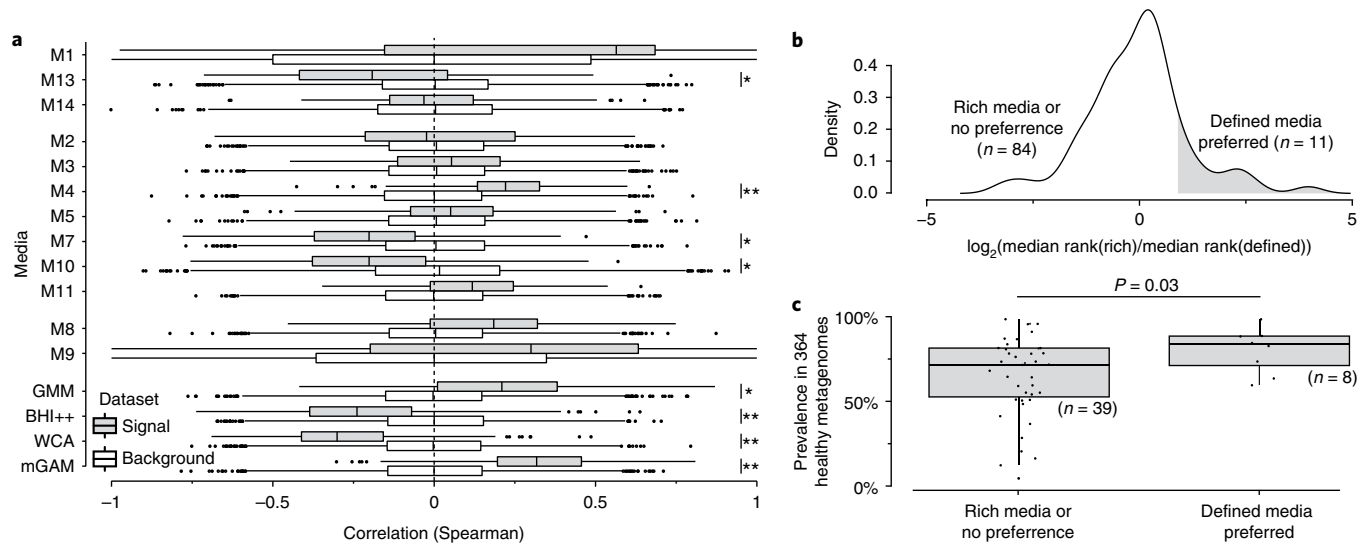

Fig. 3 | Species growth patterns provide insights into microbiota ecology. a, Distribution of correlations between bacterial average growth (58 strains) in tested media and their relative abundance within gut metagenomes of 364 healthy individuals (Methods; *P* values in Supplementary Table 6) compared to random background using two-sided Student's *t*-test (Methods). Boxplots show IQR, the median value and whiskers extending to include all the values less than 1.5 × IQR away from the 1st or 3rd quartile, respectively. $^{*}P < 0.05$ and $^{**}P < 0.05$ corrected for multiple testing (Supplementary Table 6). **b**, Distribution of $\log_2$ ratios of median ranks of species growth in rich media to that in defined media. The grey shaded area marks the region above the $\log_2$ ratio 1, which we used to identify species preferring defined media (Methods). **c**, Species with preference for defined media show significantly higher prevalence (two-sided Student's *t*-test). Only 8 out of 11 species that could be uniquely mapped in the metagenomics data are included. Boxplots show IQR, the median value and whiskers extending to include all the values less than 1.5 × IQR away from the 1st or 3rd quartile, respectively.

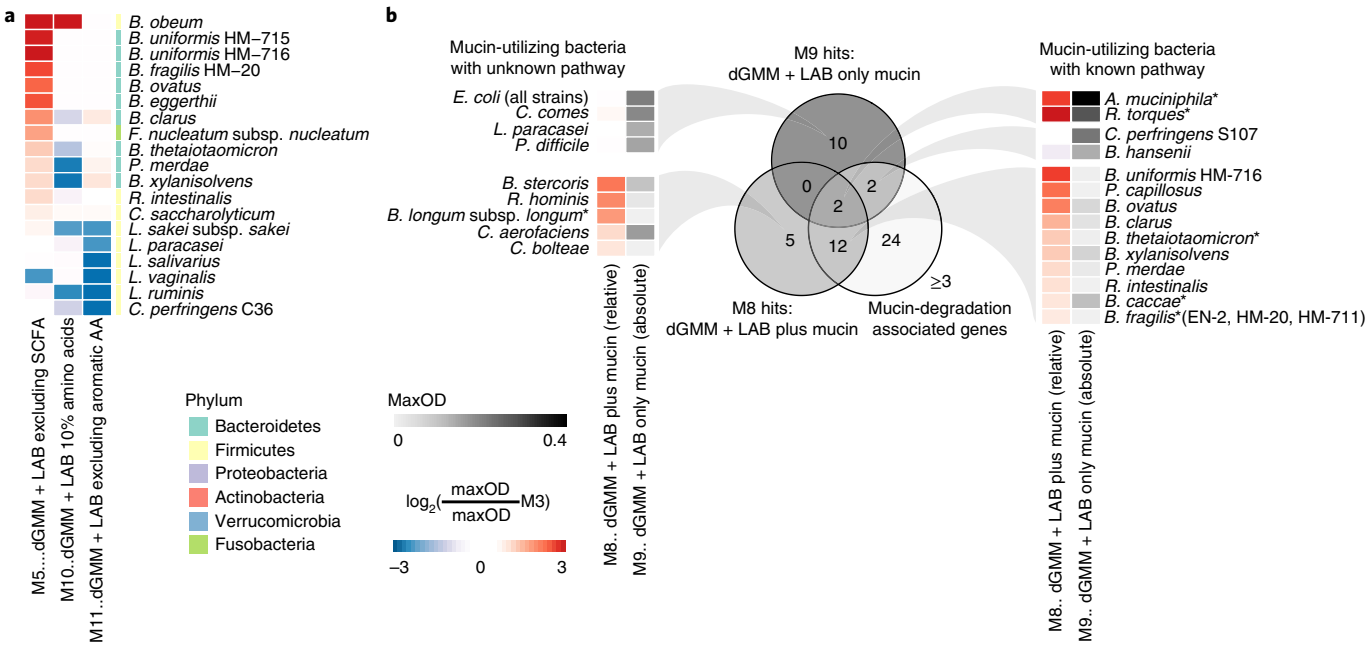

Fig. 4 | Selected metabolic characteristics of gut bacteria revealed by our screen. a, Gut bacteria inhibited or boosted in the absence of SCFAs (M5), aromatic amino acids (M11) or when the amount of amino acids was reduced to 10% (M10) compared to basis medium (M3). **b**, Overlap of species growing in the presence of mucin as the sole carbohydrate source (M9 hits), species with improved growth in the presence of additional mucin (M8 hits) (>2-fold improvement compared to the basis medium M3), and species with ≥3 known mucin degradation enzymes (based on mapping to CAZy database; Methods and Supplementary Fig. 6a,b). Strains benefiting in the presence of mucin (M8 or M9) are shown in the heatmap; *strains previously known to degrade mucin[38].

(M9 hits); two species, *A. muciniphila* and *R. torques*, overlapped between these two categories (Fig. 4b; Supplementary Fig. 6a,b), both of which have previously been reported to metabolize mucin[38]. Other known degraders, such as *B. longum* subsp. *longum*, *B. caccae*, *B. fragilis* and *B. thetaiotaomicron* were among the M8 hits. Thus, other species assigned to this category are potential, yet undescribed, mucin degraders or utilizers, including six *Bacteroides* strains, *Collinsela aerofaciens*, *Clostridium bolteae*,

Parabacteroides merdae, *Pseudoflavonifractor capillosus*, *Roseburia hominis* and *intestinalis*. Furthermore, four of these potential degraders, *B. stercoris*, *C. aerofaciens*, *C. bolteae*, *R. hominis*, are likely to use yet unknown enzymes as only few or no known genes involved in mucin-degrading pathways could be identified in their genomes (Methods, Fig. 4b and Supplementary Fig. 6a). In addition to potential active mucin degradation, part of the growth boost for some species could stem from sialic acid released from mucin (Methods; Supplementary Fig. 6c). The species that cannot degrade mucin but benefit from its degradation products like sialic acid would fall in the category of mucin utilizers. Further experiments would be necessary to clarify contribution of direct mucin degradation, sialic acid utilization and perhaps also contaminants. For example, some gut bacterial strains can degrade mucin but cannot use sialic acid[39]. We note that the growth promotion by mucin is observed only for some species, while substantial mucin degradation/impurity would be expected to cause non-specific effect throughout the screen. This supports mucin degrading/utilizing role of the species identified here. Overall, these mucin supplementation experiments suggest more widespread mucin degradation/utilization capabilities among gut bacteria than currently appreciated and presents candidate species for further investigation.

Defined media resource improves prediction of biosynthetic capabilities of gut bacteria. Defined media, in addition to permitting controlled cultivations, are a fundamental requirement for assessing biosynthetic capabilities of microorganisms. Genome-scale metabolic models can formalize this in a structured manner and allow studying effects of genetic and environmental perturbations as well as community behaviour[19,40]. Recently, a resource of 773 genome-scale metabolic models (AGORA models) of human gut bacteria was reported[15]. These cover 40 of the 96 strains growing in our screen on at least one defined medium (mucin-containing media were not considered). However, only ten of these models could recapitulate growth on our experimentally validated media (Supplementary Table 9), suggesting that currently the information used to reconstruct these models (genome sequences and literature data, with defined media available for only a few species) is insufficient for capturing major metabolic capabilities of gut bacteria. Indeed, when we used our defined media resource to improve these models (by filling the gaps in the network; Fig. 5 and Methods), we could successfully recapitulate growth on experimentally observed media for the remaining 30 species (Supplementary Table 9). The gap-filled reactions in the improved models span several metabolic pathways ranging from central carbon metabolism to vitamin biosynthesis (Supplementary Fig. 7 and Supplementary Table 9), many of which we could additionally validate using genomic evidence from the TIGRFAM gene family database[41] (Fig. 5 and Supplementary Table 9). The corresponding TIGRFAM sequence match scores are, however, only moderate—most likely due to annotation bias towards model organisms in the databases—and thus may explain why these reactions were missed in the original reconstruction. A comprehensive resource on defined media and growth requirements is thus indispensable for accurate reconstruction of metabolic models of gut bacteria.

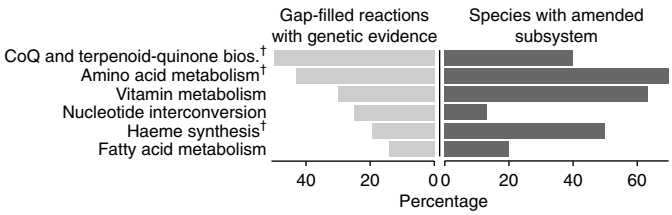

Fig. 5 | Defined media resource improves genome-scale metabolic models of gut bacteria. Metabolic reactions from several pathways needed to be added to the AGORA models[15] to recapitulate experimentally observed growth in our study (Methods). Pathway definitions are according to the AGORA model annotations. Percentage evidence for the newly added (gap-filled) reactions is based on comparison with the TIGRFAM gene family database (Methods). †Merged subsystems.

Discussion

Culture collections (such as www.atcc.org or www.dsmz.de) recommend species-specific and complex undefined media for growing individual gut bacteria. Moreover, the current knowledge on growth capabilities of such bacteria across common and defined media is sparse, and previous studies have focused on complex media and on maintaining the community diversity after cultivation[25,32,42]. We here performed a systematic evaluation of growth across a representative set of gut bacteria in several undefined rich as well as defined media. While each of the tested rich media supports growth of around 80% of the strains, defined media such as 'dGMM + LAB plus mucin' and 'dGMM + LAB excluding SCFAs' closely approach this number, supporting 70% of the tested strains.

Interestingly, differences between species in growth capacity in mGAM (a rich medium), as well as in several defined media, is correlated to their relative abundance in healthy human gut microbiomes (Fig. 3a). Together with the universality of these media, in terms of enabling growth of phylogenetically very diverse species, this opens up possibilities for systematic screening of bacteria thriving in the human gut, for example against drugs[43], and for building communities with a bottom-up approach.

The commonly held notion that most bacteria have complex metabolic requirements appears to be incorrect in the case of gut bacteria. Our results not only highlight robust growth in defined media, but also several species grow considerably better in defined than in rich media. Even within the defined media, several species preferred exclusion or reduction of SCFAs and amino acids, showing inhibitory effects of common nutrients. Although some species require SCFAs such as acetate for good growth[44], medium with no SCFAs is among the top defined media in our screen in terms of supporting a large number of strains. Such nutrient inhibitory effects can be caused by, for example, intracellular accumulation of toxic intermediates[45] or pH imbalance[46]. We further note that although we mark species–media combinations showing growth in less than half of the biological replicates as non-growing, the growth capacity in some of these cases may have been masked due to sensitivity towards difficult to control factors such as trace amounts of oxygen. The media design for isolating and cultivating hitherto uncultured gut bacterial species should thus consider, in addition to supplementing (hypothetical) missing nutrients, accounting for the toxicity of essential growth components when in excess.

The mucin-utilizing bacteria identified in this study warrant further investigations into their role in health and disease. For example, *Coprococcus comes*, which we found among the species that grow with mucin as the main carbon source (Fig. 4b, M9 hits), has been previously described to colonize the mucus layer[47]. We note that we only captured 6 out of the 10 known mucin degraders included in our study, which is likely to be due to incomplete mucin degradation pathways (utilization of intermediates only), or conditional mucin utilization in the absence of other preferred carbon sources[48]. The number of mucin-degrading species is thus likely to be much higher than presently appreciated and hence also the number of species with a role in colonic barrier integrity, which is crucial for the gut microbial ecology and respective host-microbiome interactions.

Currently available metabolic models of gut bacterial species, based on genomics and literature information of growth requirements[15], in many cases (30 out of 40; Supplementary Table 9) failed to recapitulate the growth on the defined media in our study.

This highlights the value of the presented resource for accurately assessing microbial biosynthetic capabilities. Furthermore, several cases of inconsistencies between phylogenetic and growth preference similarities, which have also been previously reported (for example, for *R. gnavus*[49]), imply that using phylogenetic relatedness alone as a guide for assessing metabolic capabilities does not suffice.

Overall, the growth media and species characterization reported here represent a resource towards an understanding of the structure and function of the human gut microbiome. We envision that this resource can be explored to facilitate metabolic modelling, and to study the effects of defined variations in nutritional conditions and xenobiotics.

Methods

Species selection. Prokaryotic species were delineated based on 40 universal, single-copy phylogenetic marker genes as previously described[50]. This species definition was shown to be in good agreement to established taxonomies[50]. Relative species abundance was quantified in 364 published faecal metagenomes of pooled asymptomatic individuals from three continents and four countries[51–54] using an approach that is based on the subset of these phylogenetic marker genes[50]. From these taxonomic abundance profiles we estimated a species core of the human gut microbiome, which included those species with a minimum prevalence of 10%, estimated by rarefying to 10,000 reads mapping to taxonomic markers, and a relative abundance of 1% or more in at least one sample. Out of 95 remaining species, we selected 45 cultivable species, isolated from human samples and preferably with an annotated genome. This equates to 58 of the selected strains. Additionally, we selected 13 probiotics, 13 pathogens, seven strains linked to colorectal cancer, IBD, foodborne diseases or bacteraemia and sepsis, one additional representative of three abundant genera, namely, *Coprococcus*, *Eubacterium* and *Prevotella*, and two strains forming separate metabolic clades (represented by EC numbers 1.4.3.4, 1.5.99.11, 2.3.1.178, 2.4.1.117, 2.7.1.14, 2.7.1.146, 2.7.1.147, 2.7.7.68, 2.7.8.28, 2.8.3.17, 3.2.1.132, 3.5.99.3, 4.1.99.2, 5.1.2.2, 6.3.2.31, 6.3.2.34; Supplementary Table 1). Enzyme gene annotations for selection of metabolically unique strains were obtained from IMG/M (Integrated Microbial Genomes and Microbiomes database; https://img.jgi.doe.gov/; accessed 18 December 2012)[55,56].

Enzyme coverage estimation. The enzyme coverage of the selected species was estimated as a ratio of the EC numbers mapping to the selected species to those mapping to the core gut microbiome species (as defined in the previous section). The EC number mapping was performed using KEGG database (KEGG Release 79.1, 1 September 2016).

Characterization of bacterial growth. Bacteria were cultivated at 37 °C under anaerobic conditions in a vinyl anaerobic chamber (COY) inflated with a gas mix of approximately 15% carbon dioxide, 83% nitrogen and 2% hydrogen. Prior to the experiment, bacteria were pre-cultivated twice using one of the following media: modified Gifu anaerobic medium broth (mGAM[29], HyServe), gut microbiota medium (GMM[25]), brain heart infusion broth (BHI, Sigma-Aldrich) supplemented with 2 mg l^{-1} ß-NAD and 0.5 mg l^{-1} haemin (BHI++), MRS (de Man, Rogosa and Sharpe, Sigma-Aldrich) + 0.05% (w/v) cysteine (MRS+), mGAM supplemented with 10 mM taurine and 60 mM sodium formate (mGAM++) or a 1:1 mixture of GMM and mGAM (GMM + mGAM) (Supplementary Table 1). For long-term storage, cryovials containing freshly prepared bacterial cultures plus 7% DMSO were tightly sealed and frozen at −80 °C.

For the exact compositions of all newly described and modified versions of media, see Supplementary Table 2. A combination of dGMM and LAB served as the basic medium (dGMM + LAB). For SCFA-containing media, most abundant SCFAs were added in physiological concentrations, such as observed in the colon[57,58]: namely, acetate (30 mM), propionate (8 mM) and butyrate (4 mM), plus isovalerate (1 mM), a branched-chain fatty acid (BCFA) and product of leucine catabolism[59,60]. For preparation of mucin-containing media, 20 g porcine gastric mucin (M1778, Sigma-Aldrich) was dissolved per litre of 10 mM phosphate buffer (pH 7.5) and autoclaved for 20 min at 121 °C. After standing overnight at room temperature, the precipitate was removed by centrifugation, and the supernatant was added to the medium to reach a final concentration of 5 g mucin per litre of medium. Porcine gastric mucin (Sigma-Aldrich) contains up to 1.5% bound and up to 0.2% free sialic acid, which is comparable to ~0.075 mg sialic acid per ml of mucin-containing medium. For preparation of sialic acid-containing medium 0.075 mg ml^{-1} sialic acid were added to the basic medium dGMM + LAB (Supplementary Fig. 6c). The pH of all defined media was adjusted to 7.

To monitor bacterial growth, pre-cultures of individual strains were diluted in PBS to obtain an OD at 578 nm of 0.5 and subsequently inoculated at OD 0.01 in 100 µl of the respective media (passage 1) in a 96 microwell plate with Nunclon Delta surface (NUNC) sealed with a Breathe-Easy sealing membrane (Sigma-Aldrich)[61].

Hourly, after thorough shaking for 1 min, growth was monitored by OD measurement at 578 nm for up to 48 h, using an Eon microplate spectrophotometer equipped with BioStack microplate stacker (BioTek) and a surrounding self-designed incubator (located within the anaerobic chamber) to allow for constant maintenance of 37 °C. For a subset of the tested conditions, we measured the pH after 48 h of cultivation (Supplementary Fig. 3) using pH indicator strips (MColorpHast, MERCK). All biological replicates (Supplementary Table 5) were performed in independent batches with newly prepared media as well as inoculums.

55 of the 96 strains (Supplementary Table 3) were further tested to control for potential nutrient carryover effects. After incubation for 48 h (passage 1), 5 µl of culture were transferred to 100 µl fresh medium twice in a row, resulting in passages 2 and 3. Measurements from only the first passage were treated as an additional biological replicate in overall growth statistics.

Purity of our bacterial stocks was regularly checked by 16S rRNA gene sequencing. Incidences of cross-contamination during the growth screen were estimated to be very low based upon two observations: (1) the screen design included wells with blank media, which showed contamination in only 0.28% of cases (2 out of 714); and (2) growth in minimal media is highly selective and reproducible indicating that well growing/robust species did not cross-contaminate.

Statistical analysis. All analysis was performed using R (version 3.2.2, www.R-project.org) and python (version 2.7.6, www.python.org). Boxplots show, unless otherwise stated, IQ, the median value and whiskers extending to include all the values less than 1.5 × IQR away from the 1st or 3rd quartile, respectively. All figures show data from biological replicates.

Growth curves analysis. Raw growth curves were first normalized with inoculum OD (BlankOD) to correct for the medium turbidity. The curves were then characterized as: (1) viable, to classify between growth or non-growth; (2) unfinished, marking when the stationary phase was not reached. The growth for the viable curves was then quantified by estimating: (1) maxOD, the maximal OD value reached; (2) rate, the growth rate measured as a slope, OD per hour; and (3) AUC, the area under the curve at 8, 12, 18 and 24 h. Where possible we used maxOD from finished growth curves only to calculate average OD. Where needed, relative growth was assessed as maxOD on particular medium divided by maxOD on dGMM + LAB medium. Furthermore, for qualitative analysis, a minimal maxOD of 0.15 was used to determine successful growth. A species was considered to grow in a given medium by applying majority rule across all biological replicates. Only data from replicates with growth phenotype were used for calculating average maxOD. Quality of the data was checked by correlating measures from corresponding biological replicates considering only measurements in agreement with majority rule: R^2 (maxOD) = 0.59.

Species clustering by growth profiles. Dissimilarity between species growth profiles were calculated using average of Euclidean distance between vectors of maxOD values on defined media (M2–M8 and M10–M11), and rich media (GMM, BHI++, WCA and mGAM). The resulting distance matrix was used for clustering with the average linkage method.

Preferential media analysis. We calculated media preference as $\log_2$ transformation fraction of median rank of species growth on rich and defined media. Preference towards defined media was stated where preference value was bigger than 1. When we required species level resolution we averaged maxOD values at species taxonomic rank.

Mucin degradation genes analysis. List of HMM models representing carbohydrate-active enzyme families (CAZy) involved in mucin degradation[38] was obtained from dbCAN[62] on 17.01.2017. HMMSCAN with default parameters was executed to check the presence of mucin genes in studied organisms (e-value < 10^{-5}, as suggested on the dbCAN webpage).

Gap-filling of genome-scale metabolic models. Metabolic models of the gut bacteria used in this study were obtained from a previous study[15]. We then used linear programming to identify minimal number of reactions missing in the model to satisfy growth phenotype (biomass yield constraint >0.1) in defined media wherein growth was experimentally observed. To further characterize the gap-filled reactions, we used EC numbers provided by the TIGRFAM (release 15) protein families annotation. We used HMMSCAN with default parameters to search for families present in organisms (e-value < 10^{-5}) and filtered matched protein families that had complete EC number assigned.

Correlation of growth with in vivo abundance. Spearman's rank correlation coefficient was used to assess correlation between core microbiome species abundances in 364 individuals and average growth (MaxOD) in each of the 16 tested media (media M15A, M15B and M16 were excluded as they did not have sufficient number of observations). Significance was assessed by calculating Wilcoxon two-sample rank sum test against subject-wise abundance permutation background.

Genomes. Translated protein sequences of studied organisms were downloaded from NCBI on 21.11.2016. For the species that did not have available genome assembly, we performed whole genome sequencing on a Illumina HiSeq 2500, with paired end reads. We removed sequencing adapters using cutadapt[63] (1.11). We assembled the resulting sequencing reads into contigs using the Spades assembler[64] (3.5.0), with k-mers sizes of 21, 33, 55 and 77. We excluded contigs with length below 200 base pairs. We annotated the resulting contigs using Prokka[65] (1.11).

Life Sciences Reporting Summary. Further information on experimental design is available in the Life Sciences Reporting Summary.

Code availability. All the code used to generate results is available online at https://github.com/sandrejev/growth_curves.

Data availability. All experimental data are provided as supplementary information. Raw data from the growth curves are available from the corresponding author upon request. For the newly sequenced genomes, the sequencing reads and annotated contigs are available in ENA with accession number PRJEB19875.

Received: 17 March 2017; Accepted: 7 February 2018;
Published online: 19 March 2018

References

1. Hooper, L. V., Littman, D. R. & Macpherson, A. J. Interactions between the microbiota and the immune system. *Science* **336**, 1268–1273 (2012).
2. Sharon, G., Sampson, T. R., Geschwind, D. H. & Mazmanian, S. K. The central nervous system and the gut microbiome. *Cell* **167**, 915–932 (2016).
3. Zeevi, D. et al. Personalized nutrition by prediction of glycemic responses. *Cell* **163**, 1079–1095 (2015).
4. Holmes, E., Li, J. V., Marchesi, J. R. & Nicholson, J. K. Gut microbiota composition and activity in relation to host metabolic phenotype and disease risk. *Cell Metab.* **16**, 559–564 (2012).
5. Sonnenburg, J. L. & Bäckhed, F. Diet–microbiota interactions as moderators of human metabolism. *Nature* **535**, 56–64 (2016).
6. Luis, A. S. et al. Dietary pectic glycans are degraded by coordinated enzyme pathways in human colonic *Bacteroides*. *Nat. Microbiol.* **3**, 210–219 (2017).
7. O'Mahony, S. M., Clarke, G., Borre, Y. E., Dinan, T. G. & Cryan, J. F. Serotonin, tryptophan metabolism and the brain-gut-microbiome axis. *Behav. Brain Res.* **277**, 32–48 (2015).
8. Bäumler, A. J. & Sperandio, V. Interactions between the microbiota and pathogenic bacteria in the gut. *Nature* **535**, 85–93 (2016).
9. Pedersen, H. K. et al. Human gut microbes impact host serum metabolome and insulin sensitivity. *Nature* **535**, 376–381 (2016).
10. Curtis, M. M. et al. The gut commensal *Bacteroides thetaiotaomicron* exacerbates enteric infection through modification of the metabolic landscape. *Cell Host Microbe* **16**, 759–769 (2014).
11. Neidhardt, F. C., Bloch, P. L. & Smith, D. F. Culture medium for enterobacteria. *J. Bacteriol.* **119**, 736–747 (1974).
12. Goodman, A. L. et al. Identifying genetic determinants needed to establish a human gut symbiont in its habitat. *Cell Host Microbe* **6**, 279–289 (2009).
13. Sebald, M. & Costilow, R. N. Minimal growth requirements for *Clostridium perfringens* and isolation of auxotrophic mutants. *Appl. Microbiol.* **29**, 1–6 (1975).
14. Lopes, J. N. & Cruz, F. S. Chemically defined media for growing anaerobic bacteria of the genus *Veillonella*. *Antonie Van. Leeuwenhoek* **42**, 411–420 (1976).
15. Magnúsdóttir, S. et al. Generation of genome-scale metabolic reconstructions for 773 members of the human gut microbiota. *Nat. Biotechnol.* **35**, 81–89 (2017).
16. Larsbrink, J. et al. A discrete genetic locus confers xyloglucan metabolism in select human gut Bacteroidetes. *Nature* **506**, 498–502 (2014).
17. Ponomarova, O. & Patil, K. R. Metabolic interactions in microbial communities: untangling the Gordian knot. *Curr. Opin. Microbiol.* **27**, 37–44 (2015).
18. Thiele, I. & Palsson, B. Ø. A protocol for generating a high-quality genome-scale metabolic reconstruction. *Nat. Protoc.* **5**, 93–121 (2010).
19. Shoaie, S. et al. Quantifying diet-induced metabolic changes of the human gut microbiome. *Cell Metab.* **22**, 320–331 (2015).
20. Castellarin, M. et al. *Fusobacterium nucleatum* infection is prevalent in human colorectal carcinoma. *Genome Res.* **22**, 299–306 (2012).
21. Strauss, J. et al. Invasive potential of gut mucosa-derived fusobacterium nucleatum positively correlates with IBD status of the host. *Inflamm. Bowel Dis.* **17**, 1971–1978 (2011).
22. Grass, J. E., Gould, L. H. & Mahon, B. E. Epidemiology of foodborne disease outbreaks caused by *Clostridium perfringens*, United States, 1998–2010. *Foodborne Pathog. Dis.* **10**, 131–136 (2013).
23. Gardiner, B. J. et al. Clinical and microbiological characteristics of *Eggerthella lenta* bacteremia. *J. Clin. Microbiol.* **53**, 626–635 (2015).
24. Könönen, E. & Wade, W. G. Actinomyces and related organisms in human infections. *Clin. Microbiol. Rev.* **28**, 419–442 (2015).
25. Goodman, A. L. et al. Extensive personal human gut microbiota culture collections characterized and manipulated in gnotobiotic mice. *Proc. Natl Acad. Sci. USA* **108**, 6252–6257 (2011).
26. Zhang, G., Mills, D. A. & Block, D. E. Development of chemically defined media supporting high-cell-density growth of lactococci, enterococci, and streptococci. *Appl. Environ. Microbiol.* **75**, 1080–1087 (2009).
27. Wegkamp, A., Van Oorschot, W., De Vos, W. M. & Smid, E. J. Characterization of the role of para-aminobenzoic acid biosynthesis in folate production by *Lactococcus lactis*. *Appl. Environ. Microbiol.* **73**, 2673–2681 (2007).
28. Evans, D. F. et al. Measurement of gastrointestinal pH profiles in normal ambulant human subjects. *Gut* **29**, 1035–1041 (1988).
29. Rettedal, E. A., Gumpert, H. & Sommer, M. O. A. Cultivation-based multiplex phenotyping of human gut microbiota allows targeted recovery of previously uncultured bacteria. *Nat. Commun.* **5**, 4714 (2014).
30. Png, C. W. et al. Mucolytic bacteria with increased prevalence in IBD mucosa augment in vitro utilization of mucin by other bacteria. *Am. J. Gastroenterol.* **105**, 2420–2428 (2010).
31. Klumpp, S., Zhang, Z. & Hwa, T. Growth rate-dependent global effects on gene expression in bacteria. *Cell* **139**, 1366–1375 (2009).
32. Browne, H. P. et al. Culturing of 'unculturable' human microbiota reveals novel taxa and extensive sporulation. *Nature* **533**, 543–546 (2016).
33. Ríos-Covián, D. et al. Intestinal short chain fatty acids and their link with diet and human health. *Front. Microbiol.* **7**, 185 (2016).
34. Louis, P., Hold, G. L. & Flint, H. J. The gut microbiota, bacterial metabolites and colorectal cancer. *Nat. Rev. Microbiol.* **12**, 661–672 (2014).
35. Bergeim, O. Toxicity of intestinal volatile fatty acids for yeast and *Esch. coli*. *J. Infect. Dis.* **66**, 222–234 (1940).
36. Hentges, D. J. Influence of pH on the inhibitory activity of formic and acetic acids for *Shigella*. *J. Bacteriol.* **93**, 2029–2030 (1967).
37. De Felice, M., Levinthal, M., Iaccarino, M. & Guardiola, J. Growth inhibition as a consequence of antagonism between related amino acids: effect of valine in *Escherichia coli* K-12. *Microbiol. Rev.* **43**, 42–58 (1979).
38. Tailford, L. E., Crost, E. H., Kavanaugh, D. & Juge, N. Mucin glycan foraging in the human gut microbiome. *Front. Genet.* https://doi.org/10.3389/fgene.2015.00081 (2015).
39. Ng, K. M. et al. Microbiota-liberated host sugars facilitate post-antibiotic expansion of enteric pathogens. *Nature* **502**, 96–99 (2013).
40. Ponomarova, O. et al. Yeast creates a niche for symbiotic lactic acid bacteria through nitrogen overflow. *Cell Syst.* **5**, 345–357 (2017).
41. Haft, D. H. et al. TIGRFAMs and genome properties in 2013. *Nucleic Acids Res.* **41**, D387–D395 (2013).
42. Lau, J. T. et al. Capturing the diversity of the human gut microbiota through culture-enriched molecular profiling. *Genome Med.* **8**, 72 (2016).
43. Maier, L. et al. Extensive impact of non-antibiotic drugs on human gut bacteria. *Nature* https://doi.org/10.1038/nature25979 (2018).
44. Duncan, S. H., Hold, G. L., Harmsen, H. J. M., Stewart, C. S. & Flint, H. J. Growth requirements and fermentation products of *Fusobacterium prausnitzii*, and a proposal to reclassify it as *Faecalibacterium prausnitzii* gen. nov., comb. nov. *Int. J. Syst. Evol. Microbiol.* **52**, 2141–2146 (2002).
45. Buurman, E. T., Pennock, J., Tempest, D. W., Teixeira de Mattos, M. J. & Neijssel, O. M. Replacement of potassium ions by ammonium ions in different micro-organisms grown in potassium-limited chemostat culture. *Arch. Microbiol.* **152**, 58–63 (1989).
46. Roe, A. J., O'Byrne, C., McLaggan, D. & Booth, I. R. Inhibition of *Escherichia coli* growth by acetic acid: a problem with methionine biosynthesis and homocysteine toxicity. *Microbiology* **148**, 2215–2222 (2002).
47. Nava, G. M., Friedrichsen, H. J. & Stappenbeck, T. S. Spatial organization of intestinal microbiota in the mouse ascending colon. *ISME J.* **5**, 627–638 (2011).
48. Sonnenburg, J. L. et al. Glycan foraging in vivo by an intestine-adapted bacterial symbiont. *Science* **307**, 1955–1959 (2005).
49. Crost, E. H. et al. Utilisation of mucin glycans by the human gut symbiont *Ruminococcus gnavus* is strain-dependent. *PLoS ONE* **8**, e76341 (2013).
50. Mende, D. R., Sunagawa, S., Zeller, G. & Bork, P. Accurate and universal delineation of prokaryotic species. *Nat. Methods* **10**, 881–884 (2013).
51. Huttenhower, C. et al. Structure, function and diversity of the healthy human microbiome. *Nature* **486**, 207–214 (2012).
52. Nielsen, H. B. et al. Identification and assembly of genomes and genetic elements in complex metagenomic samples without using reference genomes. *Nat. Biotechnol.* **32**, 822–832 (2014).
53. Qin, J. et al. A human gut microbial gene catalogue established by metagenomic sequencing: commentary. *Nature* **11**, 28 (2010).
54. Qin, J. et al. A metagenome-wide association study of gut microbiota in type 2 diabetes. *Nature* **490**, 55–60 (2012).

55. Chen, I. M. A. et al. IMG/M: Integrated genome and metagenome comparative data analysis system. *Nucleic Acids Res.* **45**, 507–516 (2017).
56. Markowitz, V. M. et al. IMG/M 4 version of the integrated metagenome comparative analysis system. *Nucleic Acids Res.* **42**, 568–573 (2014).
57. Topping, D. L. & Clifton, P. M. Short-chain fatty acids and human colonic function: roles of resistant starch and nonstarch polysaccharides. *Physiol. Rev.* **81**, 1031–1064 (2001).
58. Cook, S. I. & Sellin, J. H. Review article: short chain fatty acids in health and disease. *Aliment. Pharmacol. Ther.* **12**, 499–507 (1998).
59. Massey, L. K., Sokatch, J. R. & Conrad, R. S. Branched-chain amino acid catabolism in bacteria. *Bacteriol. Rev.* **40**, 42–54 (1976).
60. Allison, M. J. Production of branched-chain volatile fatty acids by certain anaerobic bacteria. *Appl. Environ. Microbiol.* **35**, 872–877 (1978).
61. Martens, E. C. et al. Recognition and degradation of plant cell wall polysaccharides by two human gut symbionts. *PLoS Biol.* **9**, e1001221 (2011).
62. Yin, Y. et al. DbCAN: a web resource for automated carbohydrate-active enzyme annotation. *Nucleic Acids Res.* **40**, 445–451 (2012).
63. Martin, M. Cutadapt removes adapter sequences from high-throughput sequencing reads. *EMBnet J.* **17**, 10–12 (2011).
64. Bankevich, A. et al. SPAdes: a new genome assembly algorithm and its applications to single-cell sequencing. *J. Comput. Biol.* **19**, 455–477 (2012).
65. Seemann, T. Prokka: rapid prokaryotic genome annotation. *Bioinformatics* **30**, 2068–2069 (2014).

Acknowledgements

We thank H. KleinJan and L. Maier for experimental assistance, O. Ponomarova for advice on media design and D. Machado for advice on metabolic modelling. Sequencing was performed at Genecore, EMBL. We thank Dupont Health and Nutrition (formerly Danisco Sweeteners OY, Finland) for providing *L. acidophilus* NCFM, *L. paracasei* ATCC SDS275, *B. animalis* subsp. *lactis* Bl-04 and BI-07, D. Clarke for *Shigella sonnei* 53 G and the enteropathogenic *Escherichia coli* strains CFT073, E2348/69, H10407, HM605 and UTI89, E. Denamur for the *Escherichia coli* strains ED1a and IAI1, M. Blokesch for the *Vibrio cholerae* strains A1552 and N16961, H. Andrews-Polymenis for the *Salmonella enterica typhimurium* strains CDC 6516-60 and LT2 and C. Darby for *Yersinia pseudotuberculosis* YPIII. This project has received funding from the European Union's Horizon 2020 research and innovation program under grant agreement no. 686070. MT and MP were supported by the EMBL interdisciplinary postdoctoral program.

Author contributions

M.T., P.B., A.T. and K.R.P. conceived the study. M.T., S.A., A.T. and K.R.P. designed the study. M.T., M.P., A.Z. and G.Z. selected gut bacterial strains. M.T. and M.Klünemann performed in vitro experiments. S.A. analysed data. S.A. and P.J. performed metabolic modelling. S.A. and G.Z. compiled figures. M.Kuhn contributed to in vivo abundance analysis. M.G. annotated sequenced genomes. P.B., A.T. and K.R.P. supervised the study. M.T., S.A. and K.R.P. wrote the manuscript. All authors read and commented on the manuscript.

Competing interests

A patent application has been filed based on this work.

Additional information

Supplementary information is available for this paper at https://doi.org/10.1038/s41564-018-0123-9.

Reprints and permissions information is available at www.nature.com/reprints.

Correspondence and requests for materials should be addressed to P.B. or A.T. or K.R.P.

Publisher's note: Springer Nature remains neutral with regard to jurisdictional claims in published maps and institutional affiliations.

nature research

Corresponding author(s): Peer Bork, Athanasios Typas, Kiran R. Patil

☐ Initial submission ☐ Revised version ☒ Final submission

Life Sciences Reporting Summary

Nature Research wishes to improve the reproducibility of the work that we publish. This form is intended for publication with all accepted life science papers and provides structure for consistency and transparency in reporting. Every life science submission will use this form; some list items might not apply to an individual manuscript, but all fields must be completed for clarity.

For further information on the points included in this form, see Reporting Life Sciences Research. For further information on Nature Research policies, including our data availability policy, see Authors & Referees and the Editorial Policy Checklist.

Experimental design

1. Sample size

Describe how sample size was determined.

The required number of replicates was decided based on common practice in these type of experiments. In the dataset, 1614 out of 1695 cases (96%) have 3 or more biological replicates. In particular, the dataset has 81 cases with 2 biological replicates, 1337 cases with 3 biological replicates, 69 cases with 4 biological replicates, 124 cases with 5 biological replicates, 78 cases with 6 biological replicates, 3 cases with 7 biological replicates, 2 cases with 8 biological replicates and one case with 12 biological replicates. In addition each biological replicate has at least 2 technical replicates grown on the same plate.

2. Data exclusions

Describe any data exclusions.

No samples were excluded for the final analysis. However, in cases where there was a variation in growth status (growth/no growth) within the corresponding biological replicates we calculated the mean MaxOD using only samples with the most common growth status.

3. Replication

Describe whether the experimental findings were reliably reproduced.

The data reproducibility was checked by correlating measures from biological replicates considering only replicates exhibiting the most common growth status across all corresponding replicates (R2=0.59). We concluded that this correlation shows a satisfactory reproducibility considering the expected variation in such biological assays.

4. Randomization

Describe how samples/organisms/participants were allocated into experimental groups.

Not applicable

5. Blinding

Describe whether the investigators were blinded to group allocation during data collection and/or analysis.

Not applicable

Note: all studies involving animals and/or human research participants must disclose whether blinding and randomization were used.

6. Statistical parameters

For all figures and tables that use statistical methods, confirm that the following items are present in relevant figure legends (or in the Methods section if additional space is needed).

n/a	Confirmed
☐	☒ The exact sample size (*n*) for each experimental group/condition, given as a discrete number and unit of measurement (animals, litters, cultures, etc.)
☐	☒ A description of how samples were collected, noting whether measurements were taken from distinct samples or whether the same sample was measured repeatedly
☐	☒ A statement indicating how many times each experiment was replicated
☐	☒ The statistical test(s) used and whether they are one- or two-sided (note: only common tests should be described solely by name; more complex techniques should be described in the Methods section)
☐	☒ A description of any assumptions or corrections, such as an adjustment for multiple comparisons
☐	☒ The test results (e.g. *P* values) given as exact values whenever possible and with confidence intervals noted
☐	☒ A clear description of statistics including central tendency (e.g. median, mean) and variation (e.g. standard deviation, interquartile range)
☐	☒ Clearly defined error bars

See the web collection on statistics for biologists for further resources and guidance.

Software

Policy information about availability of computer code

7. Software

Describe the software used to analyze the data in this study.	All analysis was performed using R (3.2.2) and python (2.7.6).

For manuscripts utilizing custom algorithms or software that are central to the paper but not yet described in the published literature, software must be made available to editors and reviewers upon request. We strongly encourage code deposition in a community repository (e.g. GitHub). *Nature Methods* guidance for providing algorithms and software for publication provides further information on this topic.

Materials and reagents

Policy information about availability of materials

8. Materials availability

Indicate whether there are restrictions on availability of unique materials or if these materials are only available for distribution by a for-profit company.	All bacterial strains, except those obtained from third parties (listed in the acknowledgement statement) with restricted use agreement, are available upon request.

9. Antibodies

Describe the antibodies used and how they were validated for use in the system under study (i.e. assay and species).	N.A.

10. Eukaryotic cell lines

a. State the source of each eukaryotic cell line used.	N.A.
b. Describe the method of cell line authentication used.	N.A.
c. Report whether the cell lines were tested for mycoplasma contamination.	N.A.
d. If any of the cell lines used are listed in the database of commonly misidentified cell lines maintained by ICLAC, provide a scientific rationale for their use.	N.A.

Animals and human research participants

Policy information about studies involving animals; when reporting animal research, follow the ARRIVE guidelines

11. Description of research animals

Provide details on animals and/or animal-derived materials used in the study.	N.A.

Policy information about studies involving human research participants

12. Description of human research participants

Describe the covariate-relevant population characteristics of the human research participants.	N.A.